Titel/Title: Kinematic Analysis of a Novel Parallel 2SPRR+1U Ankle Mechanism in Humanoid Robot

Autor*innen/Author(s): Shivesh Kumar, Abhilash Nayak, Heiner Peters, Christopher Schulz, Andreas Müller & Frank Kirchner

Veröffentlichungsversion/Published version: Postprint

Publikationsform/Type of publication: Buch, Monographie

Kinematic analysis of a novel parallel 2SPRR+1U ankle mechanism in humanoid robot

Shivesh Kumar[1], Abhilash Nayak[3], Heiner Peters[1], Christopher Schulz[1], Andreas Müller[4], and Frank Kirchner[1,2]

[1] Robotics Innovation Center, German Research Center for Artificial Intelligence (DFKI GmbH), Bremen 28359, Germany
shivesh.kumar@dfki.de, heiner.peters@dfki.de, christopher.schulz@dfki.de
[2] Universität Bremen, Fachbereich Mathematik und Informatik, Arbeitsgruppe Robotik, Bremen 28359, Germany frank.kirchner@dfki.de
[3] LS2N, Ecole Centrale de Nantes, Nantes 44321, France abhilash.nayak@ls2n.fr
[4] Institute of Robotics, Johannes Kepler University, Linz 4040, Austria a.mueller@jku.at

Abstract. Parallel mechanisms are increasingly being used as modular subsystems in various robots and man-machine interfaces for their good stiffness, payload to weight ratio and dynamic properties. This paper presents the kinematic analysis of a novel parallel mechanism of type 2SPRR+1U for application as a humanoid ankle joint with two degrees of freedom. Tools from computational algebraic geometry are used to provide solutions to the forward and inverse kinematics problems. These are further used to characterize the workspace of this mechanism and provide description of its singularity curves. The kinematic analysis demonstrates that the chosen design can provide human ankle like workspace and good torque transmission capability without suffering from any singularities which makes it an ideal candidate for ankle joint module in humanoid robots.

Keywords: kinematic analysis, parallel mechanisms, ankle joint, humanoids

1 Introduction

The growing popularity of parallel mechanisms includes their new applications as modular subsystems in humanoids, animaloids and man-machine interfaces due to their good stiffness, payload to weight ratio and dynamic properties. Indeed the lower amount of moving mass and freedom to place actuators away from the moving platform motivates researchers to develop new mechanisms which can better mimic the complex anatomy of biological systems. In recent years, closed loop sub-mechanisms such as Active Ankle [4], Stewart platform, 2SPU+1U [7], double parallelogram linkage [5] etc. have been used in various hybrid robotic systems like hominid CHARLIE [3], multi-legged robot MANTIS [1], RECUPERA full body exoskeleton [2] and humanoid robot LOLA [6]. Most of these hybrid robots utilize parallel submechanisms as two or three DOF orientational units.

In this paper, we present a novel two degrees of freedom orientational parallel mechanism of type 2SPRR+1U which is used as an ankle joint in a humanoid robot developed at DFKI-RIC (see Fig. 1). The kinematic actuation principle of this mechanism comprises of a motion constraint generator leg with a universal joint and two auxiliary

actuation legs of type SPRR as shown in Fig. 2. It is well known that during walking, the torque required for the pitch movement is larger than the torque required for the roll movements [6]. When the two motors are actuated in the same direction, the mechanism produces a pitch only movement demonstrating good torque transmission characteristics. It has been shown in biomechanics studies that during the ankle pitch movement of human gait, a peak torque between 105 Nm and 120 Nm is required when flexion/extension angle is between -6° and -12° [8]. To reflect this in the ankle design, the foot attachment points of the two linear actuators may be displaced along the z-axis by 30 mm. Utilizing a common universal joint at the offset points would reduce the workspace of the roll movement. Instead, two skew revolute joints, with axes parallel to axes of universal joint on constraint generator leg, connected by an intermediate offset link are used to provide the desired torque characteristics in the pitch movement with minimal influences on the motion range of roll movement. The main contribution of this paper is a comprehensive kinematic analysis of this mechanism.

The paper is organized as follows: Section 2 presents the manipulator's architecture and constraint equations. Section 3 presents the solutions to the direct and inverse kinematic problems by utilizing tools from computational algebraic geometry. Section 4 presents the workspace characterisation, description of its singularity curves and performance analysis and Section 5 concludes the paper.

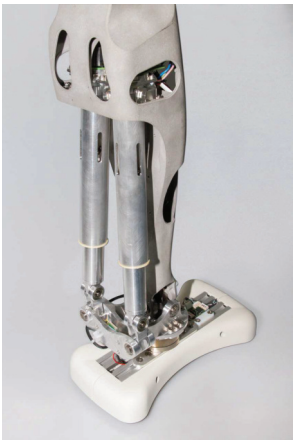

Fig. 1: Built-up prototype of Ankle joint

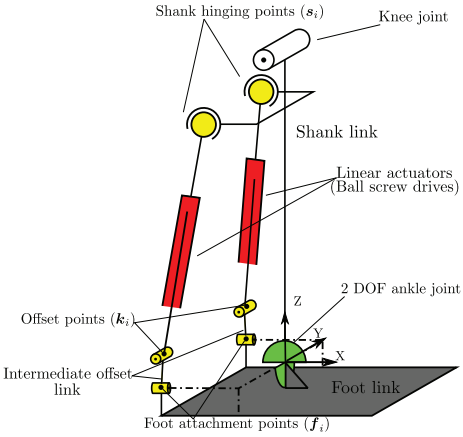

Fig. 2: Scheme of the mechanism

2 Architecture and Constraint Equations

The mobility of a mechanism ($\mathscr{M}$) can be calculated with the help of Kutzbach-Grübler criteria as follows:

$$d_s(\mathscr{M}) = s\cdot(n-m-1)+f = s\cdot(-c)+f\,, \tag{1}$$

where n is number of links in the mechanism $3+3+2=8$, m is total number of joints $4+4+1=9$, f is total dof of joints $2+6+6=14$, and s is the motion parameter. Since,

it is a spatial mechanism, $s = 6$. Hence, the mobility can be calculated as $d_s(\mathscr{M}) = 6 \cdot (8-9-1) + 14 = 2$.

The manipulator architecture and geometry is shown in Fig. 3. Let us define a set of three points: shank point ($\mathbf{s}_i$), foot attachment point ($\mathbf{f}_i$) and the offset point ($\mathbf{k}_i$) on the two auxiliary actuation legs of the mechanism. The base frame O is attached to the shank link and is coincident with the end effector (EE) frame E attached to the foot link in zero configuration. The intermediate offset link $\mathbf{f}_i\mathbf{k}_i$ rotates about the x-axis (denoted as $\hat{\mathbf{n}}$) of the frame defined at $\mathbf{f}_i$, thus point $\mathbf{k}_i$ moves on a circle of radius r equal to the length of the link, $\|\mathbf{f}_i - \mathbf{k}_i\|$. The length of the linear actuators (d_i) is the norm of the vector ($\mathbf{k}_i - \mathbf{s}_i$). We also define a vector $\boldsymbol{\delta}_i := (\mathbf{s}_i - \mathbf{f}_i)$.

The constraint equations of the manipulator are the following:

$$d_i^2 = \|\mathbf{k}_i - \mathbf{s}_i\|^2 = \|\mathbf{p}_i - \mathbf{s}_i\|^2 + \|\mathbf{k}_i - \mathbf{p}_i\|^2 \ , i \in \{1,2\} \tag{2}$$

We can rewrite (2) purely as a function of $(\mathbf{s}_i, \hat{\mathbf{n}}, \mathbf{f}_i)$.

$$\begin{aligned} d_i^2 &= \|\hat{\mathbf{n}} \cdot \boldsymbol{\delta}_i\|^2 + (\|\mathbf{f}_i - \mathbf{p}_i\| - r)^2 \\ d_i^2 &= \|\hat{\mathbf{n}} \cdot \boldsymbol{\delta}_i\|^2 + (\|\hat{\mathbf{n}} \times \boldsymbol{\delta}_i\| - r)^2 \end{aligned} \tag{3}$$

For the purpose of visualization or computing passive joint angles, it is necessary to compute the point $\mathbf{k}_i$ which is given by (4).

$$\mathbf{k}_i = \mathbf{f}_i + r\frac{\boldsymbol{\delta}_i - (\hat{\mathbf{n}} \cdot \boldsymbol{\delta}_i)\hat{\mathbf{n}}}{\|\boldsymbol{\delta}_i - (\hat{\mathbf{n}} \cdot \boldsymbol{\delta}_i)\hat{\mathbf{n}}\|} \tag{4}$$

The orientation of the moving platform is parameterized by roll (θ, around X axis) and pitch (ϕ, around Y axis) angles such that ${}^O\mathbf{R}_E = \mathrm{Rot}(X,\theta) \cdot \mathrm{Rot}(Y,\phi)$. The revolute joint axis vector ($\hat{\mathbf{n}}$) and the foot attachment point ($\mathbf{f}_i$) are expressed in global coordinate frame using $\hat{\mathbf{n}} = {}^O\mathbf{R}_E \cdot \hat{\mathbf{n}}_E$ and $\mathbf{f}_i = {}^O\mathbf{R}_E \cdot \mathbf{f}_i^E$ respectively where $\hat{\mathbf{n}}_E$ and $\mathbf{f}_i^E$ denote the revolute joint axis and foot attachment point vector in EE frame.

3 Solving Forward and Inverse Kinematics

Algebraic geometry techniques have proven to be useful in solving the forward kinematics of parallel manipulators but they require the constraint equations to be algebraic. Tangent half angle substitutions might leave the constraint equations undefined for π orientations. Hence, in order to have an algebraic description of the mechanism's constraint equations, cosines and sines are replaced by $\cos(\theta) = x$, $\sin(\theta) = y$, $\cos(\phi) = u$ and $\sin(\phi) = v$ in ${}^O\mathbf{R}_E$ though it comes at a cost of adding two more equations to the ideal set. To this end, rearranging Eq. (3) and squaring to avoid the square root term $\|\hat{\mathbf{n}} \times \boldsymbol{\delta}_i\|$ leads to four algebraic constraint equations:

$$g_1 := (d_1^2 - \|\hat{\mathbf{n}} \cdot \boldsymbol{\delta}_1\|^2 - \|\hat{\mathbf{n}} \times \boldsymbol{\delta}_1\|^2 - r^2)^2 - 4\|\hat{\mathbf{n}} \times \boldsymbol{\delta}_1\|^2 r^2 = 0 \tag{5a}$$

$$g_2 := (d_2^2 - \|\hat{\mathbf{n}} \cdot \boldsymbol{\delta}_2\|^2 - \|\hat{\mathbf{n}} \times \boldsymbol{\delta}_2\|^2 - r^2)^2 - 4\|\hat{\mathbf{n}} \times \boldsymbol{\delta}_2\|^2 r^2 = 0 \tag{5b}$$

$$g_3 := x^2 + y^2 - 1 = 0 \tag{5c}$$

$$g_4 := u^2 + v^2 - 1 = 0 \tag{5d}$$

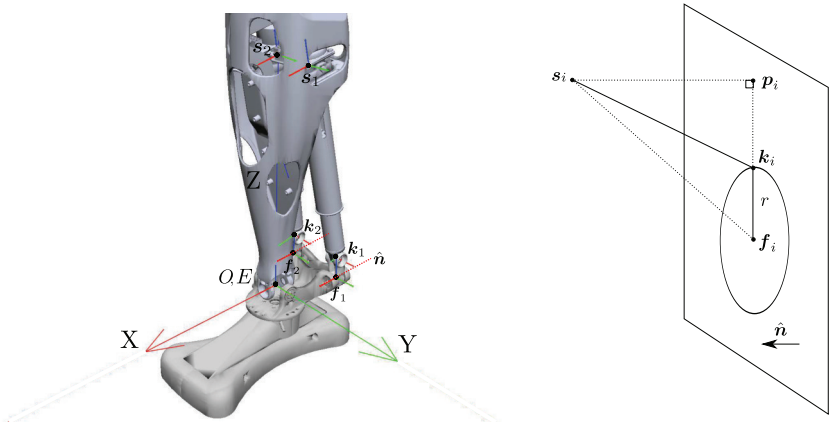

Fig. 3: Geometry of the 2 dof ankle mechanism (RGB colours denote XYZ axes)

After substituting the geometric dimensions provided in Table 1, the constraint equations are only a function of variables x, y, u, v, d_1 and d_2. g_1 and g_2 are 16 degree polynomials and are quite long to show here due to space constraints.

The solution to inverse kinematics problem (IKP) of the manipulator is straightforward and unique for a given orientation of the moving platform as the joint variables d_i can be easily calculated from Eq. (3). It is noteworthy that when the roll angle is zero, Eq. (3) yields $d_1 = d_2$.

i	$\mathbf{s}_i$	$\mathbf{f}_i^E$	$\hat{\mathbf{n}}_E$	$\|\mathbf{f}_i\mathbf{k}_i\|$
1	$(-22.30, 25, 291.27)^T$	$(-70, 40, 0)^T$	$(1,0,0)^T$	30
2	$(-22.30, -25, 291.27)^T$	$(-70, -40, 0)^T$	$(1,0,0)^T$	30

Table 1: Geometric dimensions of the ankle mechanism

The direct kinematics problem (DKP) aims to find the variables x, y, u and v when the prismatic joint lengths are specified. In search of maximum number of solutions to DKP (assembly modes), an ideal of the constraint polynomials g_i is defined: $\mathscr{I} = \langle g_1, g_2, g_3, g_4 \rangle \,|\, \mathscr{I} \subseteq k[u, v, x, y]$. Finding the Groebner basis with a pure lexicographic ordering of the orientation parameters in any order leads to a univariate polynomial of degree 32. Since squaring two of the four constraint equations quadruples the number of solutions, the number of solutions must be quartered. Hence, the upper limit to DKP solutions of the manipulator under study is eight. To investigate the number of real solutions, **RootFinding[Isolate]** function of Maple™is used. The algorithm behind this function finds out the rational univariate representation of the set of polynomials and isolates the real roots of these univariate polynomials based on Descartes' rule of sign and the bisection strategy in a unified framework. The variables d_1 and d_2 are varied from 221 mm to 331 mm (physical motion range of linear actuators) with an increment

of 6 mm and the percentage of the number of real DKP solutions is listed in Table 2. It is evident that the maximum number of real solutions for the considered set of prismatic joint lengths is six. Figure 4 shows six such assembly modes when $d_1 = 221$ mm and $d_2 = 228.3$ mm. It is speculated that a different choice of design parameters might lead to eight real solutions to DKP. In the physical construction of the ankle joint, passive joint limits are chosen such that there exists a unique solution to forward kinematics for a given input of actuator lengths in their feasible motion range (for instance Fig. 4e).

Number of solutions	0	2	4	6	8
Number of poses (/2601)	124	268	2146	63	0
Percentage	4.77	10.30	82.51	2.42	0

Table 2: Percentage of real solutions to direct kinematics

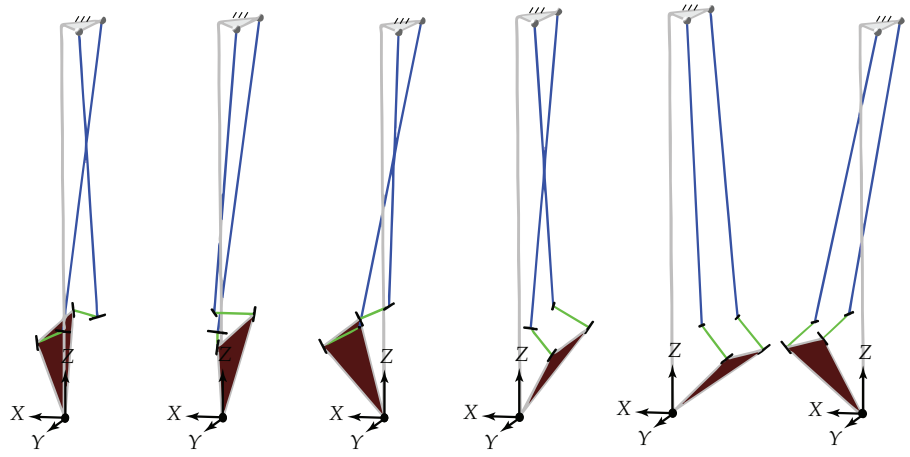

(a) $\theta = 172.32^\circ$, $\phi = -92.94^\circ$ (b) $\theta = 172.33^\circ$, $\phi = -78.30^\circ$ (c) $\theta = 175.32^\circ$, $\phi = -116.30^\circ$ (d) $\theta = 175.30^\circ$, $\phi = -54.91^\circ$ (e) $\theta = 5.03^\circ$, $\phi = 39.28^\circ$ (f) $\theta = 5.09^\circ$, $\phi = 131.92^\circ$

Fig. 4: Assembly modes for $d_1 = 221$ mm and $d_2 = 228.3$ mm

4 Workspace, Singularity and Performance Analysis

To demonstrate the suitability of the novel 2-SPRR+1U mechanism as a humanoid ankle joint, it is important to compute and characterize its feasible workspace in orientation and configuration domains. The feasible configuration space is calculated by varying the orientation variables describing foot rotation, roll (θ) and pitch (ϕ) angles, in the range $[-\pi, \pi]$. Then the physical limits of the linear actuators ($d_i \in [221, 331]$mm) are imposed to compute the workspace of the mechanism under actuator constraints. The

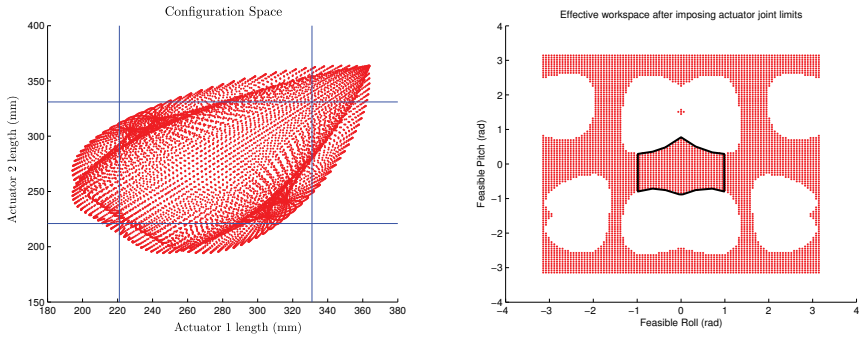

Fig. 5: Configuration space and orientation workspace under actuator physical limits

resulting configuration space and orientation workspace are shown in Fig. 5. It is possible to take into account physical limits of passive joints in the mechanism to further compute the physically realizable workspace which is indicated with a closed curve in the figure. The final range of motion (ROM) of the proposed ankle mechanism is more than that of an average human and is presented in Table 3 (compare with [8]).

The ankle mechanism under study does not have any limb singularities since the auxiliary actuation legs do not generate any constraints on the moving platform. Nonetheless, the actuation scheme results in the so called actuation singularities that can be determined through the kinematic Jacobian matrix of the manipulator obtained by the partial differentiation of the constraint polynomials in Eq. (5) with respect to the orientation parameters:

$$\mathbf{J} = \begin{bmatrix} \frac{\partial g_1}{\partial \theta} & \frac{\partial g_1}{\partial \phi} \\ \frac{\partial g_2}{\partial \theta} & \frac{\partial g_2}{\partial \phi} \end{bmatrix} \tag{6}$$

The configurations for which the determinant of the Jacobian matrix $\mathbf{J}$ vanishes are called actuation singularities. The determinant of $\mathbf{J}$ depends only on θ and ϕ. An implicit plot of the equation $\det(\mathbf{J}) = 0$ in terms of the orientation variables θ and ϕ is shown in Fig. 6 which shows the singularity curves in the mechanism's workspace. Also, it can be observed that there exist four singularities each for pure roll ($\phi = 0$) and pure pitch ($\theta = 0$) movements. Fig. 7 shows the singular poses for the pure roll and pure pitch movements which are closest to the zero configuration of the mechanism.

The quality of velocity or force transmission of a parallel manipulator can be measured by plotting the inverse of condition number of the kinematic Jacobian matrix($\mathbf{J}$) over the manipulator's workspace. The inverse of condition number of the Jacobian is calculated with $c(\mathbf{J}) = \frac{1}{\|\mathbf{J}\| \cdot \|\mathbf{J}^{-1}\|}$ where $\|\cdot\|$ represents the Euclidean norm of the matrix. From Fig. 6, it is evident that the kinematic Jacobian matrix is well-conditioned in the feasible orientation workspace of the ankle mechanism.

For practical purposes, it is crucial to calculate the maximum absolute velocity and torque available at the EE, from the maximum force and velocity that can be delivered by the actuators. These are computed with the help of kinematic Jacobian matrix

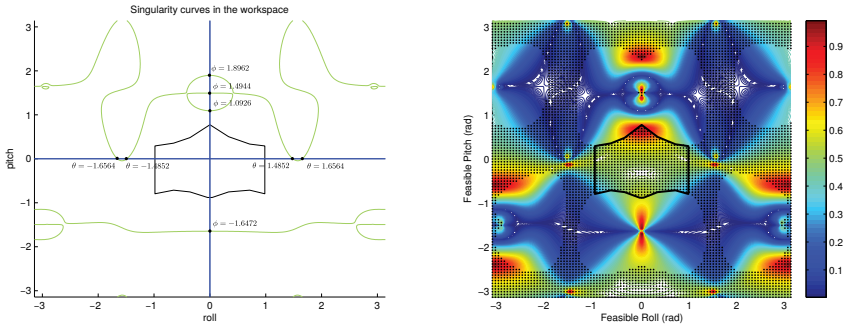

Fig. 6: Singularity curve and inverse of condition number over workspace

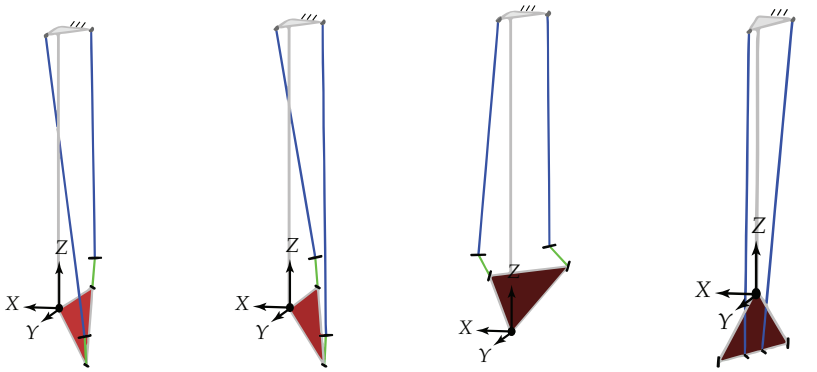

(a)	(b)	(c)	(d)
$\theta = -1.49$ rad	$\theta = 1.49$ rad	$\phi = 1.09$ rad	$\phi = -1.65$ rad
$d_1 = 306$ mm	$d_1 = 228$ mm	$d_1 = 216$ mm	$d_1 = 362$ mm
$d_2 = 228$ mm	$d_2 = 306$ mm	$d_2 = 216$ mm	$d_2 = 362$ mm

Fig. 7: Singularity configurations for pure roll (θ) and pure pitch (ϕ) movements

and actuator specification (see Table 3). The proposed ankle design is light weight and provides good force and velocity transmission characteristics along pure pitch and roll movements which are highly desired in modern humanoid robots.

5 Conclusion

This paper presents a comprehensive kinematic analysis of a novel 2SPRR+1U parallel mechanism for application as a humanoid ankle joint with two degrees of freedom. Using tools from computational algebraic geometry, an upper bound to the number of solutions to the direct kinematics problem and the real assembly modes have been studied. Inverse kinematics is used to study the mechanism's workspace, compute the singularity curves and quality of velocity and force transmission. From the study, it is clear that the ankle mechanism is highly suitable for application as a humanoid ankle sub-

Range (min. to max.)	Position	Max. abs. force	Max. abs. velocity
Ankle pitch	-51.5° to 45°	43.8 N m to 110.1 N m	$61\,^\circ\,\mathrm{s}^{-1}$ to $154^\circ\,\mathrm{s}^{-1}$
Ankle roll	-57° to 57°	30.6 N m to 57 N m	$118\,^\circ\,\mathrm{s}^{-1}$ to $222^\circ\,\mathrm{s}^{-1}$
Linear actuator	221 mm to 331 mm	754 N	$81\,\mathrm{mm\,s}^{-1}$

Table 3: Ankle joint specification (total weight of lower leg = 3.2 kg, weight of one actuator = 0.44 kg)

system module. The analysis presented in this work can be easily applied to 2SPU+1U mechanism by substituting $r = 0$.

Acknowledgement

The work presented in this paper was performed within the project TransFIT, funded by the German Aerospace Center (DLR) with federal funds from the Federal Ministry for Economic Affairs and Energy (BMWi) (Grant Nos. 50RA1701, 50RA1702 and 50RA1703). The fourth author acknowledges that this work has been partially supported by the Austrian COMET-K2 program of the Linz Center of Mechatronics.

References

1. Bartsch, S., Manz, M., Kampmann, P., Dettmann, A., Hanff, H., Langosz, M., v. Szadkowski, K., Hilljegerdes, J., Simnofske, M., Kloss, P., Meder, M., Kirchner, F.: Development and control of the multi-legged robot mantis. In: International Symposium on Robotics (2016)
2. Kirchner, E.A., Will, N., Simnofske, M., Benitez, L.M.V., Bongardt, B., Krell, M.M., Kumar, S., Mallwitz, M., Seeland, A., Tabie, M., Whrle, H., Yksel, M., He, A., Buschfort, R., Kirchner, F.: Recupera-reha: Exoskeleton technology with integrated biosignal analysis for sensorimotor rehabilitation. In: Transdisziplinre Konferenz SmartASSIST, pp. 504–517 (2016)
3. Kuehn, D., Bernhard, F., Burchardt, A., Schilling, M., Stark, T., Zenzes, M., Kirchner, F.: Distributed computation in a quadrupedal robotic system. International Journal of Advanced Robotic Systems **11**(7), 110 (2014)
4. Kumar, S., Bongardt, B., Simnofske, M., Kirchner, F.: Design and kinematic analysis of the novel almost spherical parallel mechanism active ankle. Journal of Intelligent & Robotic Systems (2018). URL https://doi.org/10.1007/s10846-018-0792-x
5. Kumar, S., Simnofske, M., Bongardt, B., Mueller, A., Kirchner, F.: Integrating mimic joints into dynamics algorithms exemplified by the hybrid recupera exoskeleton. In: Advances In Robotics (AIR-2017), June 28 - July 2, New Delhi, India. ACM-ICPS (2017)
6. Lohmeier, S., Buschmann, T., Schwienbacher, M., Ulbrich, H., Pfeiffer, F.: Leg design for a humanoid walking robot. In: 2006 6th IEEE-RAS International Conference on Humanoid Robots, pp. 536–541 (2006)
7. Serracn, J., Puglisi, L., Saltaren, R., Ejarque, G., Sabater-Navarro, J., Aracil, R.: Kinematic analysis of a novel 2-d.o.f. orientation device. Robotics and Autonomous Systems **60**(6), 852 – 861 (2012)
8. Zoss, A.B., Kazerooni, H., Chu, A.: Biomechanical design of the berkeley lower extremity exoskeleton (bleex). IEEE/ASME Transactions on Mechatronics **11**(2), 128–138 (2006)